
**POLİTEKNİK DERGİSİ**

***JOURNAL of POLYTECHNIC***

ISSN: 1302-0900 (PRINT), ISSN: 2147-9429 (ONLINE)

URL: http://dergipark.gov.tr/politeknik

# Design and implementation of a Thrust Vector Control (TVC) test system

# *Bir İtki Vektör Kontrol (İVK) test sistemi tasarımı ve uygulaması*

***Yazar(lar) (Author(s))**: Ahmet ÜNAL[1], Kemal YAMAN[2], Emre OKUR[3] ve Mehmet Arif ADLI[4]*

*ORCID[1]: 0000-0001-5483-3188*

*ORCID[2]: 0000-0003-3063-391X*

*ORCID[3]: 0000-0002-3101-9041*

*ORCID[4]: 0000-0002-3223-064X*

**Bu makaleye şu şekilde atıfta bulunabilirsiniz(To cite to this article)**: Ünal A., Yaman K., Okur E. ve Adlı M.A., "Design and implementation of a Thrust Vector Control (TVC) test system", ***Politeknik Dergisi***, 21(2): 497-505, (2018).

**Erişim linki (To link to this article):** http://dergipark.gov.tr/politeknik/archive

**DOI:** 10.2339/politeknik.404009

# Bir İtki Vektör Kontrol (İVK) Test Sistemi Tasarımı ve Uygulaması

***Araştırma Makalesi / Research Article***

**Ahmet ÜNAL[1]*, Kemal YAMAN[1], Emre OKUR[1] , Mehmet Arif ADLI[2]**

[1] The Scientific and Technological Research Council of Turkey-Defense Industries Research and Development Institute, (TÜBİTAK SAGE) 06261, Ankara, Turkey

[2] Gazi University, Graduate School of Natural and Applied Sciences, Department of Mechanical Engineering, 06500, Turkey

(Geliş/Received : 25.01.2017 ; Kabul/Accepted :25.02.2017 )

**ÖZ**

Roket motorları, üretilen itki kuvvetine bağlı olarak performanslarının değerlendirilmesi için statik olarak test edilmektedir. Roket motoru statik test değerlendirmesinin en önemli parametrelerinden biri motorun ürettiği itki değeridir. Üretilen itki, yük hücreleri ile donatılmış bir yapısal eleman olan İtki Vektör Kontrol (İVK) Ölçüm Sistemi kullanılarak ölçülür. Bu çalışmada, katı yakıtlı roket motorunun itki performansını ölçmek için bir yük sensörü sistemi tasarlanmıştır. Test sisteminde, altı serbestlik derecesine göre roket motorunun ateşleme boyunca üretmiş olduğu kuvvetler ve momentler ölçülmüştür. Elde edilen deneysel sonuçların ve analiz sonuçlarının birbiriyle uyumlu olduğu görülmektedir. Tasarlanan stand, 50 [kN]'a kadar eksenel itki üreten roket motorların eksenel itkisini, yanal (yanlış hizalanmış) itki bileşenlerini ve yuvarlanma momentini ölçebilmektedir.

**Anahtar Kelimeler: İtki vektör kontrol, itki ölçümü, roket motoru, test standı, sonlu elemanlar.**

# Design and Implementation of a Thrust Vector Control (TVC) Test System

**ABSTRACT**

The rocket engines are tested statically to evaluate the performance of engine based upon thrust produced. One of the most important parameters of the rocket engine static testing evaluation is to measure the thrust produced by the engine. The thrust produced is measured using a Thrust Vector Control (TVC) test system which is a structural element equipped with load cells. In this study, a load sensor system was designed to measure the propulsion performance of a solid propellant rocket motor. The forces and moments of the rocket motor with respect to the six degrees of freedom of the test system were measured during firing. It is seen that the obtained experimental results and the analysis results are compatible with each other. The designed stand is capable of measuring axial thrust and lateral (misaligned) thrust components, and the rolling moment for rocket motors producing axial thrust up to 50 [kN].

**Keywords: Thrust vector control, thrust measurement, rocket motor, test stand, finite elements**

## 1. INTRODUCTION

Measurements related to performance and reliability of thrust systems are necessary at the stages of development, evaluation and verification of design are required. One of the tests done in this context is static firing test. The main variables measured during the static firing tests are the thrust force, the combustion chamber pressure and various temperature data [1-3]. There are various methods for thrust measurement such as direct force measurement, measurement of exit properties of exhaust gases and momentum balance establishment. The most common feature of these methods is using direct force measurement that requires a special mechanism. The mechanisms for measuring force which are called “Thrust Measurement System” are basically composed of a fixed lattice, a mobile carrier system, support columns, load cells and a calibration system. In the literature Brimhall [4, 5] et al. developed a six degree of freedom (DOF) solid rocket test stand. The plant is used by university groups and commercial companies who want to stay in the Cape Canaveral Air Force Station, and primarily, to acquire approval of their engines for a government approved shuttle flight. This thrust stand has been developed by the Florida Institute of Technology to provide reliable static motor testing for solid rockets with the collaboration of Florida and US Air Force 45th Spacewalk (45th SW). By using this device, the torque of the stand, axial thrust, orthogonal (misaligned) thrust components and solid motors that produce a thrust force of up to 44500 N (10000 lb) can be measured. The data collection system of the thrust stand consists of five sensors for both thrust categories. The Thrust Category 1 consists of 4,45 [kN] (1000 lb) engines. The Thrust Category 2 consists of larger engines producing a thrust of 4,45 [kN] (1000 lb) to 44,5 [kN] (10000 lb).

Gligorijevic et al. [6] constructed a special TVC system in order to measure the side thrust force. They reported that the results obtained from the developed system are

**Sorumlu Yazar (Corresponding Author)*
*e-posta : ahmet.unal@tubitak.gov.tr*

consistent with the numerical (CFD) results. Wekerle at al. [7], present a new TVC system for new Brazilian launch vehicles. They develop a high performance, closed-loop servo hydraulic actuator controlled TVC system. The dynamic responses of TVC system were determined experimentally and its mathematical model was derived. Experimental results show a satisfactory consistence with the proposed model. However, the models have to be verified with non-linear joint stiffness of the flexible nozzle. Unlike classical TVC design, some studies similar to the 6-DOF hexagon mechanism are also found in the literature [8]. The results show that a TVC system, which can accurately measure the thrust of a rocket motor, requires at least 3-DOF degrees of freedom. In the work of Milos et al., the designed hexagon-shaped TVC platform can be used to test very low thrust systems, but considering the high thrust case it does not yield reliable results due to low strength of frame.

Nowadays, solid propellant rocket engines have been replaced by hybrid systems [9-11]. In the Prince et al's [9] study "L" type ground test system was used to measure the thrust of a hybrid rocket. The ground test was performed in an "L" configuration. That is, the oxidant tank was suspended in an S-load cell to measure the oxidant mass flow rate, and the oxidizer passed through a smooth 90-degree curve to pass horizontally through the flight ball valve to the combustion chamber. Thus, the combustion chamber was bolted to the floor with a load cell around the front of the combustion cell for propulsion measurement, supported by a horizontal structure. The cold flow tests were continued until the desired mass flow rate was reached and then the actual hot fire occurred. Wright et al. [10] developed a laboratory scale, 6-DOF, hybrid-TVC system. The thrust stand proved to be stable during calibration tests. Thrust force vector components and roll, pitch, and yaw moments were calculated for test firings with an oxygen mass flow rate in the range of 0,0174–0,0348 kg $s^{-1}$.

In micro scale, under the vacuum condition a new micro thrust test stand was developed by Wang et al. [11]. Similarly, a new test stand with a very high sensitivity, which can feel a small push at 0,1N, was designed by Lugini and Romano [12]. According to the ballistic pendulum principle, the test system is suspended in the air. Acceleration is measured precisely according to the amount of movement back and forth and right to left during the experiment.

The test ramps developed on the macro scale [13, 14] as opposed to the micro scale are mostly used in in space shuttle design research. Smiley et al. [13] developed a macro scale TVC for a rocket system (Dream Chaser/Atlas V) to launch into space. This test program was included in the Dream Chaser design process. As a result of the test, the information that will have critical preliminaries in the overall development of the thrust system architecture is gained.

In this study, a TVC Performance Test System has been developed to determine axial and lateral thrust of a rocket motor with thrust vector control. The data obtained from the TVC Performance Test System shall be used as input to the guidance control of the ammunition used by the solid propellant rocket motor. Therefore, improving the sensitivity of the test system plays a critical role. A dynamic model of the system with computer aided PATRAN-NASTRAN and MATLAB software have been created. The dynamic model will, in real terms, be influential inputs to the TVC Performance Test System. Outputs of the dynamic model will be compared to the static firing test data. As a result of comparison, findings for improvement will be reflected in the real system. Here some theoretical relation will be given with respect to static loads for conceptual design of TVC test system shown in Fig. 1.

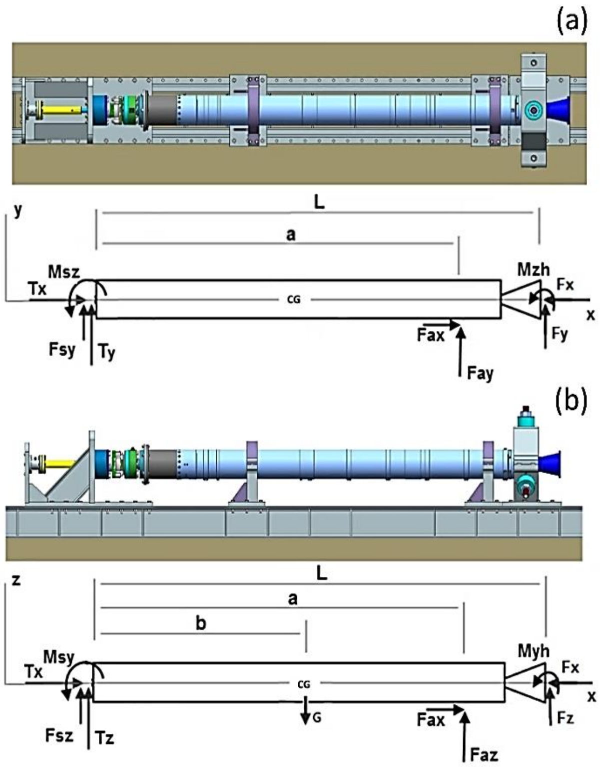


**Figure 1.** TVC test system static loading boundary conditions in (a) *z-x* plane and (b) *x-y* plane

In x-y plane the static equilibrium equations can be written as follows:

$$\sum F_x = 0:\ T_x + F_{ax} - F_x = 0 \quad (1)$$

$$\sum \boldsymbol{F_y} = \boldsymbol{0}:\ \boldsymbol{T_y} + \boldsymbol{F_{sy}} + \boldsymbol{F_{ay}} + \boldsymbol{F_y} = \boldsymbol{0} \quad (2)$$

$$\sum \boldsymbol{M_z} = \boldsymbol{0}:\ \boldsymbol{M_{sz}} + \boldsymbol{a}\,\boldsymbol{F_{ay}} + \boldsymbol{L}\boldsymbol{F_y} + \boldsymbol{M_{zh}} = \boldsymbol{0},\ (\boldsymbol{M_{sz}} = \boldsymbol{0},\ \boldsymbol{M_{zh}} = \boldsymbol{0}) \quad (3)$$

In *x-z* plane,

$$\sum \boldsymbol{F_z = 0}: \boldsymbol{T_z + F_{sz} + F_{az} - G + F_z = 0} \quad (4)$$

$$\sum \boldsymbol{M_z = 0}: \boldsymbol{M_{sz} - bG + a\, F_{az} + LF_z + M_{zh} = 0}, \; (\boldsymbol{M_{sz} = 0, M_{zh} = 0}) \quad (5)$$

The horizontal and lateral forces on sensors ($F_{ay}$ and $F_{az}$) can be determined by the following equations:

$$F_{ay} = -(F_{left} \cos 30° - F_{right} \cos 30°) \quad (6)$$

horizontal lateral force on sensors and,

$$F_{az} = -(F_{right} \sin 30 + F_{left} \sin 30° - F_{top}) \quad (7)$$

vertical lateral force on sensors.

Lateral thrust measurement is mainly based on the data and calculations obtained from reaction forces. For the lateral thrust component occurring in the *x-y* plane the Eq. (3) is used and for the component formed in the *x-z* plane the Eq. (5) is used. The unknown reaction forces of $F_{ay}$ and $F_{az}$ are determined from the measurements of sensors placed at an angle of 120 degrees using Eq. (6) and Eq. (7). The moment values of the friction generated in the joint are neglected because they are very small. Other unknown parameters are taken from the results of rocket engine combustion analysis as fuel weight *G* and location of fuel center of gravity *b*.

## 2. MATERIALS AND METHOD

The thrust stand given in Fig. 2 is designed to test a wide range of rocket motors, including engines with diameters up to 290 mm and lengths up to 3,5 m. The concrete pad has to be at least 3,5 m long to adjust the largest engine and to fixed a set of threaded bars. In this way, the back of structure can be carried to any of the holes, in which all motor spacings are provided. On top of the concrete base there are two basic structures: backward sensor structure and forward sensor structure (Fig. 2).

The forward structure is designed to withstand the axial thrust of the solid propellant rocket motor.

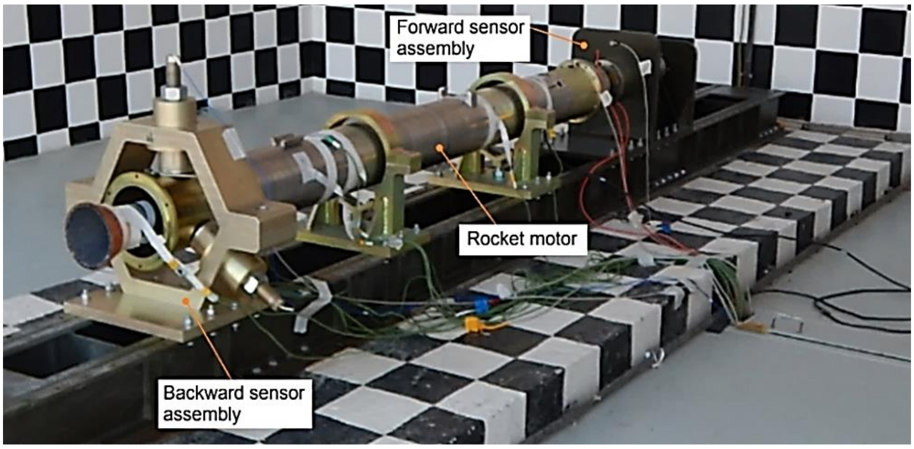


**Figure 2.** Instrumented final test Stand assembly

Moving plates in the forward direction allow small adjustments to the motor alignment in the *x* and *y* directions. The universal joint used in the system eliminates measurement errors caused by possible angular misalignment between the motor and forward structure. In other words, by using this connection, load measurement is always provided in the axial load, but moment load is prevented. It also provides ease of installation (See Fig. 3).

A loadcell and a torque sensor is installed between the front end of the engine and the forward structure to measure axial thrust and torque. The measuring devices and sensors used in the tests are listed in Table 1

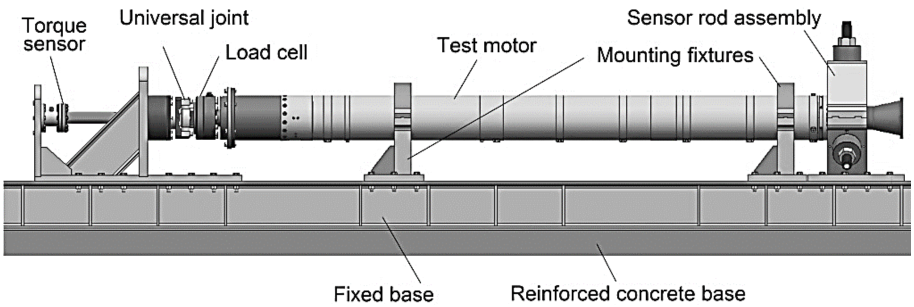


**Figure 3.** CAD model of TVC test system and its components

**Table 1.** Measuring devices and equipment used in experiments

| Device and equipment | Brand-Model | Type | Capacity | Precision | # |
|---|---|---|---|---|---|
| Load cell | HBM-U10M | Strain-gage | 50 [kN] | 2 [mV/v] | 1 |
| Force sensor | PCB 208-A14 | ICP type | 4,448 [kN] | 1124 [mV/kN] | 3 |
| Data acquisition system | NI_PXIe-1073 CHASSIS and NI_PXI-4462 module | AC/DC coupling | with 4 canals | - | 1 |

The backward sensor structure consists of a steel plate and a fixed base. The back structure is floated in the guideways as the moving part of the shoe while the forward structure has a permanent mounting. The fixed support acts like a collar holding the motor. The three devices (Sensing arms), which are placed at 120° intervals in the fixed rest, can be adjusted to the center of the station and allow it to be centered between 50 mm and 290 mm diameter as shown in Figure 4.

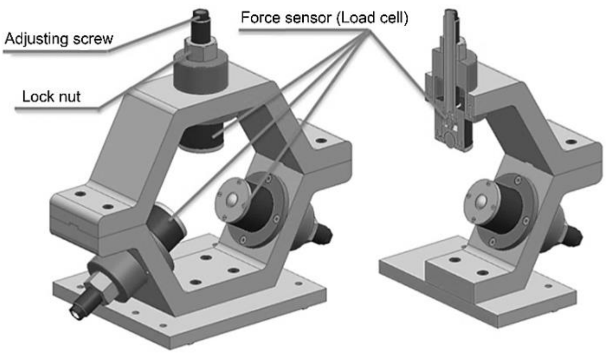


**Figure 4.** CAD model of sensing rods assembly

The arms include a single axis piezoelectric force sensor that measures the motor thrust misalignment. The use of bearings in this frame provides a relatively frictionless contact surface between the back structure and the motor.

The coefficient of friction of spherical transfer elements at the beginning of motion is generally in the range of 0,01-0,015 [15]. If it is assumed that the side impact is 10 times lower than the axial thrust, the spherical transfer element and the axial load measurement can be made with about 0,1% uncertainty. A sensing and data acquisition system is used in the thrust stand to obtain thrust and moment data. The detection system consists of five sensors or transducers placed in such a way as to allow six degrees of freedom. Remember from the design review, a force transducer and torque converter are fixed between the front-end section of the motor and the adjustment plates of the front structure.

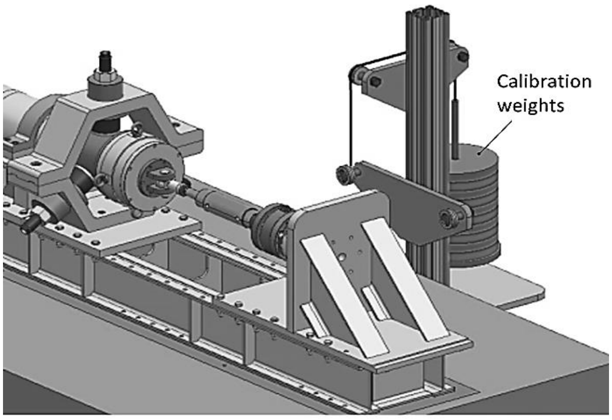


**Figure 5.** Calibration setup

The calibration test setup is a measurement system in which the TVC system equipped with all gauges is calibrated with static loads before testing. This calibration system also should be checked for performing the verification properly before the test. The calibration adapter and other auxiliary parts according to the dimensions of the motor body which will be used for calibration purposes are shown in Fig. 5. Axial thrust is simulated by means of a hydraulic piston, and both lateral thrust and rolling moment can be created with the help of hooks. Thus, the system is verified by comparing the forces and moments applied to the system with the data obtained from the test system.

For preparing the dynamic model PATRAN® and NASTRAN® finite element analysis software were used. Before the analysis, the mass-spring models of whole system were drawn. The rocket motors and adapters models are defined as a one-dimensional beam element.

In Figure 6a CAD model and applied boundary condition of sensing rod assembly and in Figure 6b its FEM mesh model is given respectively. In the finite element model, 467707 10-node TET10 solid elements and 48 RBE2-type multi-point constraint rigid elements for bolts and rigid connections are used. In addition, one RJOINT multi-point delimited element is used to model the articulated model.

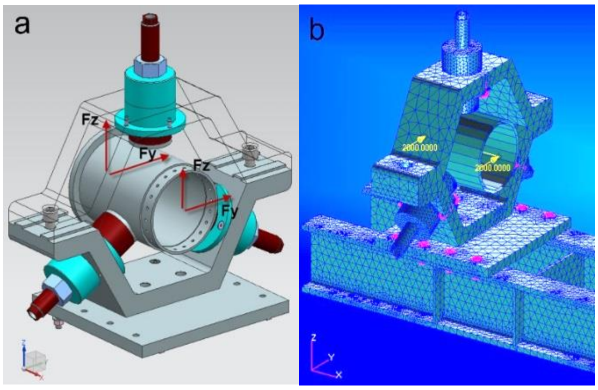


Figure 6. (a) CAD and (b) FEM-mesh model of sensing rods assembly

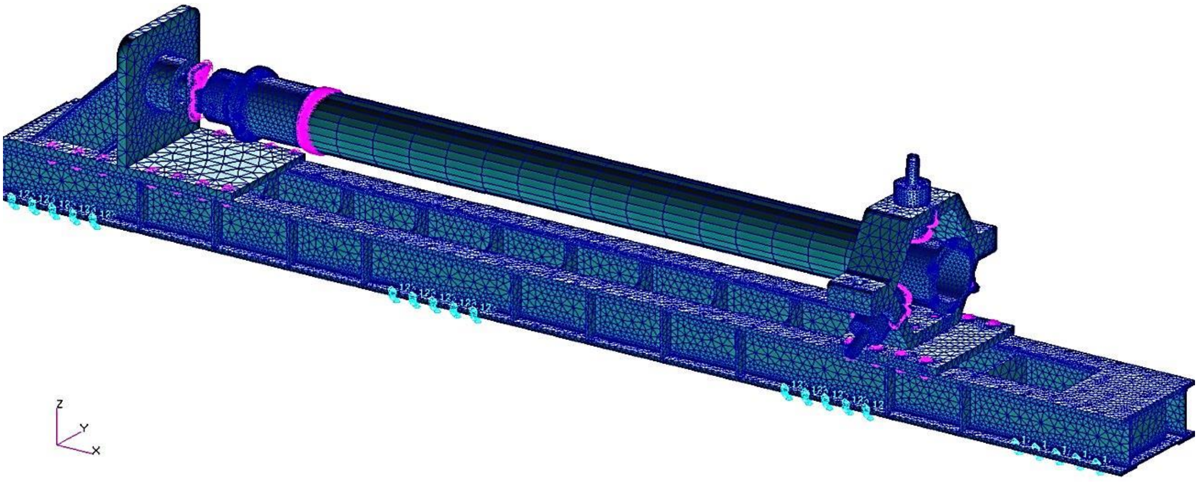

**Figure 7**. FEMs of TVC system

**Table 2.** Material properties used in analyzes [16]

| Materials | Elasticity, *E* [GPa] | Poisson ratio,*v* | Density [kg/m$^3$] | Yield stress [MPa] | Components |
|---|---|---|---|---|---|
| Aluminum (AA 6061) | 68,3 | 0,33 | 2710 | 241 | Sensor rod assembly |
| Steel (AISI/SAE 4140) | 207 | 0,30 | 7830 | 1210 | Test motor fitting parts |
| Steel (S235XX) | 210 | 0,30 | 7850 | 235 | Fixed base, torque sensor assembly, mounting fixtures |

The test motor is modeled as a one-dimensional beam element (Fig. 7)

TVC performance test assembly parts consist of steel and aluminum material. In the analyzes, the materials are modeled as linear elastic. Table 2 gives the materials and their properties used in the analyzes.

## 3. RESULTS

Axial and lateral thrust is measured during static firing test. Angles of horizontal, vertical and lateral force are computed using gained test results. These angles are used for input as thrust vector into the program. In Fig. 8 the high-speed camera image of rocket motor plume is given during the thrust test.


**Figure 8**. High-speed camera image of rocket nozzle plume during the test

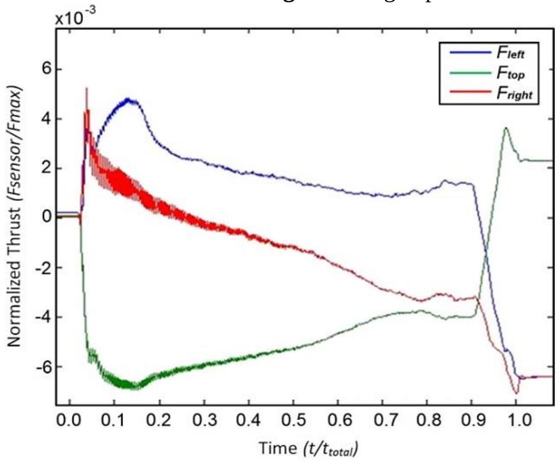


**Figure 9**. Thrust variation with time obtained from lateral thrust sensors

According to the data acquired from the sensors given in Figure 9. The reaction forces coming from the support point A formed vertically and horizontally were calculated using Eq. (6) and Eq. (7) using the data given in Fig. 9. In Fig. 10a shows a normalized curve from the *x*-axis longitudinal load cell mounted to the front end. And in Figure 10b, the compared lateral thrust components obtained using Eq. (3) and Eq (5) (See in Section 1).

In the normalization procedure, the instant thrust value read during the process is divided by the maximum thrust (*x* axis) value. As can be clearly seen from the thrust-time graphs, the thrust reaches its maximum value in a short time, i.e. about 0,05 unit time from the zero-thrust level and remains approximately horizontal for about one-unit time at this peak value. At about 0,9 unit time, thrust value suddenly falls back to zero. The similar results were obtained with Smiley et al. [13].

As a consequence of this, the rocket motor produced a stable thrust during combustion. It can be easily seen in Fig. 10b that, $F_x$ is about 100 times greater than $F_z$ and 250 times greater than $F_y$. Therefore, the most significant parameter that effect the TVC test stand design is the axial force.

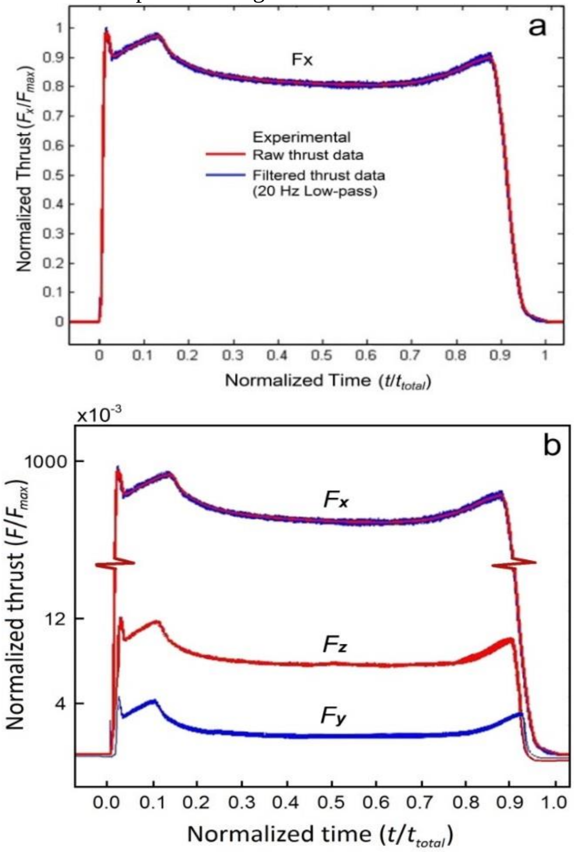


**Figure 10**. Thrust variation with time for (a) axial force ($F_x$) and (b) comparison of lateral-y ($F_y$) and lateral-z ($F_z$) with axial force ($F_x$)

In normalization procedure, the instant thrust value read during the process is divided by the maximum thrust (*x* axis) value. As can be clearly seen from the thrust-time graphs, the thrust reaches its maximum value approximately 0,05 unit time from the zero-thrust level and remains horizontally between 0,2 and 0,8 normalized time at this peak value. At about 0,9-1,0 normalized time interval, thrust value suddenly falls back to zero. The similar results were obtained with Smiley et al. [13]. As a consequence of this, the rocket motor produced a stable thrust during combustion. It can be easily seen in Fig. 10b that, $F_x$ is about 100 times greater than $F_z$ and 250 times greater than $F_y$. Therefore, the most significant parameter that effect the TVC test stand design is the axial force.

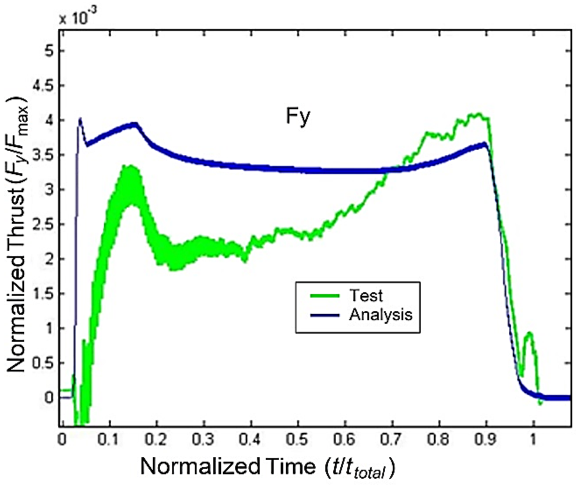


(a)

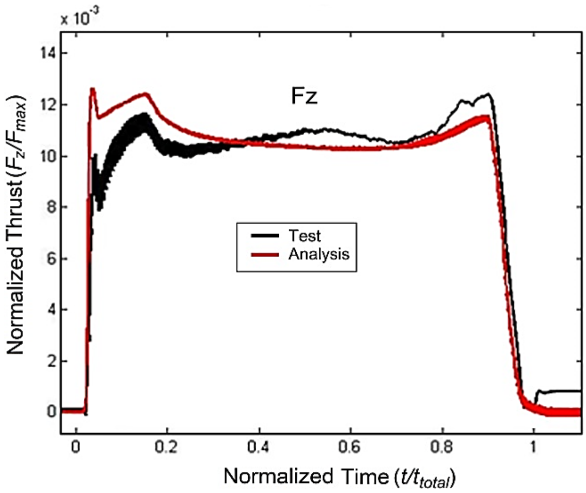


(b)

**Figure 11**. Comparison of the measured thrust to the results obtained from the analysis for (a) $F_y$ and (b) $F_z$

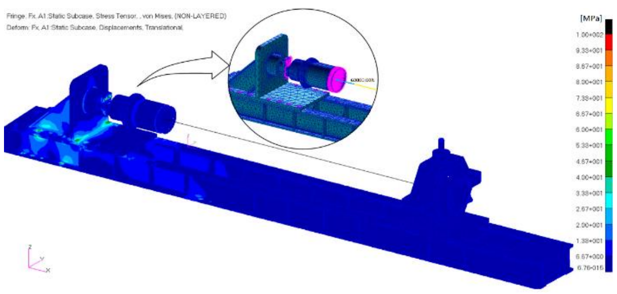

**Figure 12.** Von Mises stress distribution results of TVC test assembly according to axial thrust BC

In Figure 11a and 11b lateral-*y* and lateral-*z* thrust loads are shown respectively. The measured axial load value is used as input in analysis. The lateral thrust values in the directions of *y* and *z* are calculated by finite element analysis. The FEA results and experimental measurement results are close to each other. The sources of systematic error in these tests and any test on the thrust stand were due to the uncertainties of the sensors, the distortion of the signal due to the discharge time constant, the drift in

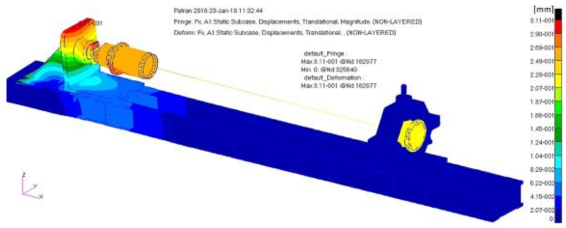

**Figure 13.** Deformation distribution results of TVC assembly according to axial thrust BC (x100 magnification)

the signal and the uncertainty in the load cell. All sensors have an uncertainty of one percent of the applied load. The test has shown an uncertainty of only 0,00001 percent; which can be neglected.

The TVC performance test system was subjected to strength analyzes using the axial force of 50 [kN], the lateral thrust forces of 4 [kN] (See Fig. 1), the boundary conditions and the finite element models are given in Fig. 6 and Fig. 7. The stress values observed in the front support subjected to axial reinforcement are around 60 [MPa] (Fig. 12).

The deformation values of the front support when the axial thrust is applied are also shown (Fig. 13). The tensile values of the whole lateral thrust sensor and the base plate exposed to the lateral thrust are very low as expected, i.e. 25 [MPa] (Fig. 14). No structural failures are observed in these tensile strengths

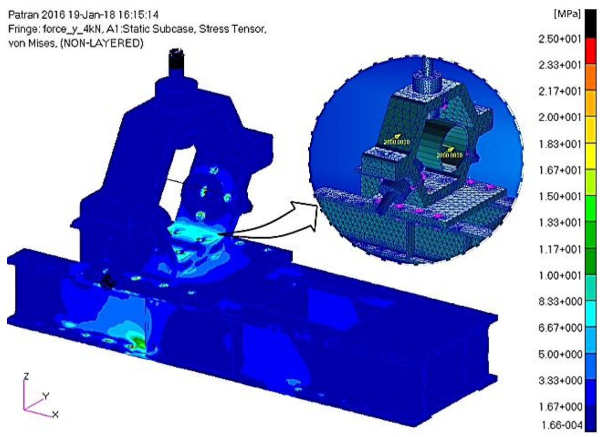


**Figure 14.** Von Mises stress distribution results of TVC test assembly according to lateral thrust BC

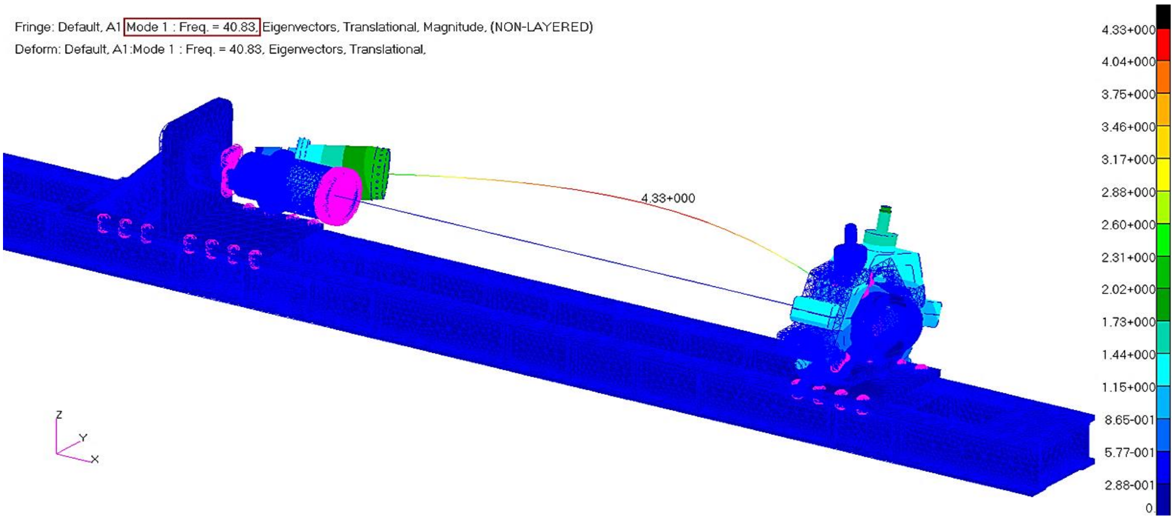


**Figure 15.** Modal analysis results of TVC assembly

Moreover, in the modal analyzes performed together with the whole test motor, the first natural frequency of the test stand is seen around 40 [Hz] (See Fig 15). This value is taken into account when filtering the test data.

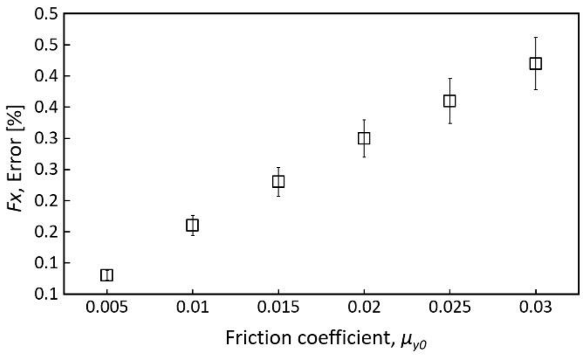


**Figure 16.** Change of the axial thrust measurement error by the spherical transfer element friction coefficient

The measurement uncertainty which may occur in the axial thrust measurement is calculated to be in the interval of friction coefficient $\mu_{yo}$=0,00-0,03 using Eq. (1), the maximum measurement uncertainty was obtained as 0,45% (Fig. 16)

## 4. CONCLUSION

In this study, a new six degree-of-freedom thrust sensor system was designed, constructed, calibrated and tested using TÜBİTAK SAGE rocket motor infrastructure in Ankara. The thrust stand proved to be stable during firing tests. The results indicate that, thrust misalignment increase due to the nonhomogeneous wear of nozzle throat. Thrust force vector components and roll, pitch, and yaw moments were calculated during the test. The test results showed that the designed and manufactured TVC test system can be easily and reliably used for accurate measuring of the rocket motor thrust for all six degrees of freedom. Experimental results and analysis results are found to be in harmony with each other. On the other hand, it was also found that the thrust-time relationship observed in experiments was consistent with the literature and the thrust behavior of the tested rocket motor was stable.

## SYMBOLS

| | |
|---|---|
| $F_x$ | :True axial thrust |
| $T_x$ | :Measured axial thrust |
| $F_{ax}$ | :The frictional force generated at the support A |
| $\mu_{yo}$ | :The frictional coefficient of the spherical transfer element |
| $T_y$ | :Horizontal reaction force in front support |
| $F_{sy}$ | :Horizontal force generated from friction by joint |
| $F_{ay}$ | :Lateral force at the support A |
| $F_y$ | :Lateral thrust (*y*-axis) component |
| $M_{sz}$ | :Moment generated from friction (*z*-axis) in joint |
| $a$ | :Distance between the reference point (joint center) and point A support |
| $L$ | :Distance between reference point and reference point of thrust vector |
| $M_{zh}$ | :Hinge moment (*z*-axis) component on the jet wings |
| $T_z$ | :Vertical reaction force on front support |
| $F_{sz}$ | :Vertical force originating from friction in joint |
| $F_{az}$ | :Vertical reaction force at the point A support |
| $F_z$ | :Lateral thrust force *z*-axis (vertical) component |
| $G$ | :Rocket motor fuel weight |
| $b$ | :The distance of the rocket motor fuel center of gravity to the reference point |

$M_{sy}$ :Moment generated from friction (*y*-axis) in joint

$M_{yh}$ :Hinge moment (*y*-axis) component on the jet wings

## ACKNOWLEDGMENTS

Special thanks to TÜBİTAK SAGE for providing the Rocket Motor Test Infrastructure.

## REFERENCES

[1] Runyan R.B., Rynd J.P., Seely J.F., "Thrust stand design principles", ***AIAA 17th Aerospace Ground Testing Conference***, July 6-8, Nashville, TN, USA, (1992).

[2] Turner M.J.L., Rocket and spacecraft propulsion. Principles, Practice and new development (Third edition), ***Springer-Praxis Publishing Co.***, U.K, (2009).

[3] Mattingly J.D., Elements of propulsion: Gas turbines and rockets, ***AIAA Publishing Inc.***, Virginia, USA, (2006).

[4] Brimhall Z.N., Atkinson J.P., Kirk D.R., Peebles H.G., "Design of a novel six degree of freedom solid rocket motor test stand", ***AIAA 2007-5331 43rd AIAA/ASME/SAE/ASEE Joint Propulsion Conference & Exhibit***, July 8-11, Cincinnati, OHI, USA, (2007).

[5] Brimhall Z.N., Divitotawela N., Atkinson J.P., Kirk D.R., Peebles H.G., "Design of a novel six degree of freedom solid rocket motor test stand", ***AIAA 2007-5331 44th IAA/ASME/SAE/ASEE Joint Propulsion Conference & Exhibit***, July 21-23, Hartford, CT, USA, (2008).

[6] Gligorijevic N., Zivkovic S., Subotic S., Kozomara S., Nikolic M., Citakovic S., "Side force determination in the rocket motor thrust vector control system", ***Scientific Technical Review***, 63(1): 27-38, (2013).

[7] Wekerle T., Barbosa E.G., Batagini C.M., Costa L.E.V.L., Trabasso L.G., "Closed-loop actuator identification for Brazilian Thrust Vector Control development", ***IFAC-PapersOnLine***, 49(17): 468–473, (2016).

[8] Milos P., Davidovic N., Jojic B., Milos M., Todic I., "A novel 6 DOF thrust vector control test stand", ***Tehnicki Vjesnik-Technical Gazette***, 22(5): 1247-1254, (2015).

[9] Prince E.R., Krishnamoorthy S., Ravlich I., Kotine A., Fickes A.C., Fidalgo A.I., Freeman K., Anderson K., Gerson D., "Design, analysis, fabrication, ground-test, and flight of a two-stage hybrid and solid rocket", ***AIAA 49th Joint Propulsion Conference***, July 14-17, San Jose, CA, USA, (2013).

[10] Wright A.M., Wright A.B., Born T., Strickland R., "A six degree-of-freedom thrust sensor for a labscale hybrid rocket", ***Meas. Sci. Technol***, 24: 125104 (10 pp), (2013). DOI:10.1088/0957-0233/24/12/125104.

[11] Wang A., Wu H., Tang H., Liu Y., Liang X., "Development and testing of a new thrust stand for micro-thrust measurement in vacuum conditions", ***Vacuum***, 91: 35-40, (2013).

[12] Lugini C., Romano M., "A ballistic-pendulum test stand to characterize small cold-gas thruster nozzles", ***Acta Astronautica***, 64: 615-625, (2009).

[13] Smiley M., Veno M., Bell R., "Commercial crew development—round one, milestone 3: Overview of Sierra Nevada Corporation's hybrid motor ground test", ***AIAA 47th AIAA/ASME/SAE/ASEE Joint Propulsion Conference & Exhibit***, 31 July-03 August, San Diego, CA, USA, (2011).

[14] Sunakawa H., Kobayashi T., Okita K., "Development status of electrical valve control system for LE-9 engine", ***AIAA Propulsion and Energy Forum***, 10-12 July, Atlanta, GA, USA, (2017).

[15] Alwayse Engineering Ball Transfer Unit Catalogue, https://www.alwayse.co.uk/brochures/CAT14August2015Revisions.pdf., website visit date: 15.08.2015.

[16] Granta-mi, Material Library, https://www.grantadesign.com/products/mi/index.htm, website visit date: 03.07.2016.